BBA - Molecular Basis of Disease xxx (xxxx) xxx–xxx

Contents lists available at ScienceDirect

BBA - Molecular Basis of Disease

journal homepage: www.elsevier.com/locate/bbadis

Hydrogen sulfide attenuates oxidative stress-induced NLRP3 inflammasome activation via S-sulfhydrating c-Jun at Cys269 in macrophages

Zhe Lin[a], Naila Altaf[a], Chen Li[a], Mei Chen[a], Lihong Pan[a], Dan Wang[a], Liping Xie[a], Yuan Zheng[b], Heling Fu[b], Yi Han[c], Yong Ji[a,*]

[a] Key Laboratory of Cardiovascular and Cerebrovascular Medicine, Key Laboratory of Targeted Intervention of Cardiovascular Disease, Collaborative Innovation Center for Cardiovascular Disease Translational Medicine, Nanjing Medical University, Nanjing 211166, China
[b] Animal Core Facility of Nanjing Medical University, Nanjing 211166, China
[c] Departments of Geriatrics, the First Affiliated Hospital of Nanjing Medical University, Nanjing 210029, China

ARTICLE INFO

Keywords:
Oxidative stress
Hydrogen sulfide
S-sulfhydration
NLRP3 inflammasome
Macrophages

ABSTRACT

Oxidative stress and inflammation are closely related to cardiovascular diseases. Although hydrogen sulfide (H_2S) has been shown to have powerful anti-oxidative and anti-inflammatory properties, its role in macrophage inflammation was poorly understood. The aim of this study was to investigate the role of H_2S in the regulation of macrophage NLRP3 inflammasome activation. We reported here that H_2S attenuated hydrogen peroxide (H_2O_2)-induced NLRP3 inflammasome activation, which led to caspase-1 activation and IL-1β production in macrophages. Moreover, H_2S exerted its protective effects by lowering the generation of mitochondrial reactive oxygen species (mtROS). Mechanistically, S-sulfhydration of c-Jun by H_2S enhanced its transcriptional activity on SIRT3 and p62, which contributed to the decrease of mtROS production. S-sulfhydration sites are investigated by site directed mutagenesis. Findings showed that S-sulfhydrated c-Jun exerted its protective influences via a c-Jun Cys269-dependent manner. Moreover, the protective effects of H_2S were absent in macrophage from SIRT3 knockout mice. In conclusion, these results demonstrate that H_2S attenuates oxidative stress-induced mtROS production and NLRP3 inflammasome activation via S-sulfhydrating c-Jun at cysteine 269 in macrophages.

1. Introduction

Cardiovascular diseases and their consequences are the most serious health problems worldwide [1]. In general, oxidative stress and inflammation are closely related to cardiovascular diseases, including atherosclerosis, ischemia-reperfusion injury, cardiomyopathy, and heart failure [2,3]. Moreover, the concept of oxidative stress and chronic inflammation as part of the pathophysiology of cardiovascular diseases has been accepted [4]. The excessive increase in reactive oxygen species (ROS) generation is pivotal in the progression of cardiovascular diseases [5,6]. Monocytes/macrophages are involved in the pathogenesis of atherosclerosis, aortic aneurysm, and heart diseases [7–11]. Additionally, monocytes/macrophages have been found to be diagnostic, prognostic, or therapeutic targets in cardiovascular diseases [7,12]. Macrophage infiltration and oxidative stress play a vital role in the progression of cardiovascular diseases [4,13–16].

The NLRP3 inflammasome is composed of the NLRP3(NACHT, LRR and PYD domains-containing protein 3), the adaptor protein ASC (apoptosis-associated speck-like protein containing a CARD), and caspase-1 [17]. The activation of caspase-1 by NLRP3 inflammasome contributes to the processing and secretion of the proinflammatory cytokines IL-1β and IL-18, which contribute to the so-called sterile inflammation response [18,19]. To date, several studies have indicated that NLRP3 inflammasome is activated through three possible pathways, including reactive oxygen species (ROS), intracellular potassium (K^+) concentration, and the disruption of the lysosomal membrane [20,21]. Macrophage NLRP3 inflammasome activation has been suggested to be involved in cardiovascular diseases [22–28].

Abbreviations: ANOVA, analysis of variance; BMM, bone marrow-derived macrophages; BSA, bovine serum albumin; CVD, cardiovascular diseases; DAPI, 4′,6-diamidino-2-phenylindole; DMSO, dimethyl sulphoxide; DHE, dihydroethidium; EDTA, ethylenediaminetetraacetic acid; FBS, fetal bovine serum; HEPES, 4-(2-hydroxyethyl)-1-piperazineethanesulfonic acid; H_2S, Hydrogen sulfide; H_2O_2, Hydrogen peroxide; HRP, horseradish peroxidase; IL-1β, interleukin-1β; M-CSF, macrophage colony-stimulating factor; MMTS, methyl methanethiosulfonate; mtROS, mitochondrial reactive oxygen species; NLRP3, NLR family pyrin domain containing 3; PBS, phosphate buffered solution; p62, sequestosome 1; PMA, 4β-phorbol-12-myristate-13-acetate; PVDF, polyvinylidene fluoride; RIPA, radio immunoprecipitation assay; ROS, reactive oxygen species; SDS-PAGE, sodium dodecyl sulfate polyacrylamide gel electrophoresis; SIRT3, Sirtuin 3

* Corresponding author at: Key Laboratory of Cardiovascular and Cerebrovascular Medicine, Key Laboratory of Targeted Intervention of Cardiovascular Disease, Collaborative Innovation Center for Cardiovascular Disease Translational Medicine, Nanjing Medical University, 101 Longmian Avenue, Jiangning District, Nanjing, 211166, Jiangsu, China.
E-mail address: yongji@njmu.edu.cn (Y. Ji).

https://doi.org/10.1016/j.bbadis.2018.05.023
Received 17 March 2018; Received in revised form 18 May 2018; Accepted 28 May 2018

Hydrogen sulfide (H_2S) is a gaseous transmitter and plays important roles in several diseases [29,30]. H_2S is a biologically active gas that is synthesized naturally by three enzymes, cystathionine γ-lyase (CSE), cystathionine β-synthetase (CBS) and 3-mercaptopyruvate sulfurtransferase (3-MST) [31]. In addition, H_2S acts as an endogenous scavenger for reactive oxygen species [32–34]. Furthermore, H_2S physiologically modifies protein cysteines to form S-sulfhydration, which appears to be a physiologic posttranslational modification for proteins [29,35]. Our previously studies have demonstrated that H_2S has powerful antioxidative and anti-inflammatory properties in several pathological process, including myocardial fibrosis, endothelial dysfunction, diabetes-accelerated atherosclerosis, myocardial hypertrophy, and testicular dysfunction [36–40].

In this study, exogenous treatment with H_2O_2, a ROS-generating agent, was used to mimic oxidative stress in macrophages. We demonstrated that H_2S attenuated H_2O_2-induced NLRP3 inflammasome activation in macrophages THP-1. H_2O_2-induced NLRP3 inflammasome activation led to caspase-1 activation and IL-1β production. We further demonstrated that NLRP3 bound to ROS-generated mitochondria in macrophages exposed to H_2O_2. However, pretreatment with H_2S reduced these above effects of H_2O_2 on macrophages. In addition, we found that H_2S enhanced c-Jun transcriptional activity directly via S-sulfhydration of c-Jun protein at cysteine 269. The increased c-Jun transcriptional activity contributed to the increasing expression of SIRT3 and p62, which exhibited remarkable antioxidant and anti-inflammatory effects in macrophages. This study deepens our understanding of the protective effects of H_2S via c-Jun S-sulfhydration in macrophages.

2. Materials and methods

2.1. Cell culture and treatment

THP-1 human monocyte cells obtained from Cell Bank at the Chinese Academy of Sciences were cultured in 25 mM HEPES-buffered RPMI 1640 (Life Technologies, Rockville, MD, USA) containing 10% FBS (Life Technologies, Rockville, MD, USA) and 50 μM β-mercaptoethanol (Life Technologies, Rockville, MD, USA). THP-1 cells were differentiated into macrophages by incubation with 5 ng/mL 4β-phorbol-12-myristate-13-acetate (PMA; Biyuntian, Hangzhou, China) for 24 h. RPMI 1640 complete medium was replaced before addition of H_2S donor, NaHS (100 μM; Sigma-Aldrich, St Louis, MO, USA). After 4 h treatment, cells were incubated in freshly prepared medium containing H_2O_2 (250 μM; Sigma-Aldrich, St Louis, MO, USA) for a further 4 h. Mitochondria-targeted antioxidant Mito-TEMPO was purchased from Abcam (ab144644, Cambridge, MA, USA). Cathepsin B inhibitor CA-074Me was purchased from Bachem (4027913, Bubendorf, Switzerland). $P2X_7$ receptor inhibitor A438079 was purchased from Selleck Chemicals (S7705, Shanghai, China). For cell experiments, these reagents were dissolved in dimethyl sulfoxide (DMSO) and were used at the desired concentration (indicated in figure legends).

2.2. Transient transfection and dual-luciferase reporter assay

Human c-Jun (Gene ID: 3725) cDNA was purchased from GENEWIZ, Inc. (Suzhou, China). Human c-Jun cDNA was cloned into pcDNA3.1 by GENEWIZ. Single mutation at cysteine-99 (C99A), cysteine-269 (C269A), or cysteine-320 (C320A) in c-Jun was conducted by GENEWIZ. pAP1-TA-luc vector is a luciferase reporter construct with multiple AP-1 (TGACTAA) response elements and purchased from Biyuntian (Hangzhou, China). The response elements of c-Jun in SIRT3 and p62 genes promoter were predicted via using JASPAR databases (Supplementary data 1). The wild type and deletion of the c-Jun response element in the SIRT3 and p62 promoter were purchased from GENEWIZ, Inc. (Suzhou, China). SIRT3-WT (−500−−1), $SIRT3_{\Delta-337--325}$, p62-WT (−500−−1), and $p62_{\Delta-389--377}$ were subcloned into luciferase reporter vector pGL4 (Promega, Madison, WI, USA) by GENEWIZ. pGL4.74 (Promega, Madison, WI, USA) vector was also purchased from Promega. After incubation with 5 ng/mL PMA for 24 h, THP-1 macrophages were transfected with indicated plasmids by using Lipofectamine 3000 reagent (Invitrogen) according to manufacturer's recommendations and the method as previously described [37]. Cells were cultured for 24 h after transfection. The luciferase activity was measured by the dual luciferase assay system (Promega, Madison, WI, USA) according to the manufacturer's instructions. Data were normalized by the activity of Renilla luciferase. Mcrophages were transfected with NLRP3 siRNA (sense 5′-GUUUGACUAUCUGUUCUdTdT-3′ [41]; GenePharma, Shanghai, China) using Lipofectamine 3000 (Invitrogen, Carlsbad, CA, USA) according to the manufacturer's instructions.

2.3. Western blotting

RIPA lysis buffer (Biyuntian, Hangzhou, China) containing protease inhibitor cocktail (ThermoFisher, Waltham, MA, USA) was used to obtain whole-cell lysates from macrophages. Protein concentrations were quantified using BCA Protein Assay Kit (Pierce, Rockford, IL, USA). Equal amounts of protein were loaded into SDS-PAGE and transferred onto a PVDF membrane (Bio-Rad, Hercules, CA, USA). Membranes were incubated with rabbit antibodies to caspase-1 (#3866, CST, Danvers, MA, USA), IL-1β (#ab45692, Abcam, Cambridge, MA, USA), CBS (#ab135626, Abcam), CSE (#ab151769, Abcam), NLRP3 (#13158, CST), SIRT3 (#2627, CST), and GAPDH (#AP0063, Bioworld, Nanjing, China) as well as mouse antibodies to caspase-1 p20 (#AG-20B-0048, AdipoGen, San Diego, CA, USA), 3-MST (#sc-374,326, Santa Cruz Biotechnology, Santa Cruz, CA, USA), and p62 (#MB9009, Bioworld). All blots were overlaid with appropriate HRP-conjugated secondary antibodies and visualized by enhanced chemiluminescence substrate (Bio-Rad, Hercules, CA, USA).

2.4. Immunofluorescent staining and confocal microscopy

THP-1 monocyte cells were seeded on glass slides (NEST, Wuxi, China) and incubated with 5 ng/mL PMA for 24 h. Then, the cells were treated as described above. After the treatment, the cells were washed twice with sterile PBS and fixed with ice-cold methanol, permeabilized with 0.01% Triton X-100 and blocked in 3% BSA. The cells were then incubated overnight with primary antibodies, including anti-NLRP3 (#AG-20B-0014, AdipoGen, San Diego, CA, USA), anti-caspase-1 (#3866, CST), and anti-c-Jun (#9165, CST). For experiments that used mitotracker, cells were stained with 5 μM MitoTracker Deep Red FM (#M22426, Life Technologies) for 20 min prior to methanol fixation. Secondary fluorescent antibodies (Alexa-488, or -594; Life Technologies) were added for 1 h and DAPI (#sc-24,941, Santa Cruz) was used for nuclear counterstaining. Samples were imaged through confocal microscope (Zeiss LSM 410, Oberkochen, Germany) and quantified using Image-Pro Plus analysis software.

2.5. Measurement of ROS and mtROS formation

Superoxide production in cells was detected by dihydroethidium (DHE; Vigorous, Beijing, China) assay as the manufacturer's instructions. Briefly, macrophages were treated as described above, after which the cells were washed twice with PBS and incubated with 5 μM of DHE for 30 min and washed twice with PBS. Fluorescence was measured with a Nikon TE2000 Inverted Microscope and quantified using Image-Pro Plus analysis software. Mitochondrial ROS were measured using MitoSOX (#M36008, Molecular Probes, Carlsbad, CA, USA). Briefly, macrophages were treated as above described, after which the cells were washed twice with PBS and loaded with 5 μM of MitoSOX and 100 nM MitoTracker Green FM (#M7514, Molecular Probes) for 20 min. Fluorescence was measured through confocal microscope (Zeiss

LSM 410) and quantified using Image-Pro Plus analysis software.

2.6. Modified biotin switch assay of S-sulfhydration

Modified biotin switch assay was performed as described by Ju et al. [42]. Briefly, cells were lysed in HEN buffer (250 mM HEPES (pH 7.7), 0.1 mM neocuproine, and 1 mM EDTA) supplemented with 150 μM deferoxamine, 1% NP-40, and protease inhibitor cocktail (ThermoFisher). Samples were sonicated and centrifuged at 16,000 *g* for 15 min at 4 °C. Protein concentrations of the supernatant samples were quantified using BCA Protein Assay Kit (Pierce). Lysates were diluted to reach 2 mg/mL final protein concentration and were added to blocking buffer (HEN buffer adjust to 2.5% SDS and 20 mM MMTS (methyl methanethiosulfonate)) at 50 °C for 30 min with frequent vortexing. The MMTS was then removed by acetone and the proteins were precipitated at −20 °C for 20 min. Proteins were resuspended in HENS buffer (HEN buffer containing 1% SDS) and 4 mM biotin-HPDP (*N*-[6-(biotinamido)hexyl]-3′-(2′-pyridyldithio) propinamide). After incubation for 2 h at 25 °C, biotinylated proteins were purified by streptavidin-agarose beads (ThermoFisher), which were then washed with HENS buffer. The biotinylated proteins were eluted in 2× Laemmeli sample buffer and subjected to western blotting analysis with anti-c-Jun antibody. The used chemicals were purchased from Sigma-Aldrich (St Louis, MO, USA).

2.7. Real-time PCR

Total RNA was extracted using TRIzol reagent (Takara, Dalian, China). Total RNA was reverse transcribed to cDNA by using the PrimeScript RT Master Mix Kit (Takara, Dalian, China). Real-time PCR was carried out with the resulting cDNAs in triplicate using SYBR Green remix (Takara, Dalian, China) and the ABI 7500 Real-Time PCR System (Applied Biosystems, Foster City, CA, USA). GAPDH was used for normalization. Primers' sequences are obtained from PrimerBank (pga.mgh.harvard.edu/primerbank). (PrimerBank ID: SIRT3, 157671925c1; p62, 214830450c1; GAPDH, 378404907c1) in supplementary data 1.

2.8. Animals and murine macrophage cells culture

SIRT3$^{-/-}$ mice were the gift of Professor Hongliang Li (Wuhan University, Wuhan, China) [37]. All animal experiments were approved by the Committee on Animal Care of Nanjing Medical University. Peritoneal macrophages were harvested from the peritoneal cavity with a cold RPMI 1640 medium. After centrifugation at 1200 rpm for 10 min at 4 °C, the cell pellet was washed once and resuspended in a complete medium: 25 mM HEPES-buffered RPMI 1640 (Life Technologies, Rockville, MD, USA) containing 10% FBS (Life Technologies, Rockville, MD, USA), 100 IU/mL penicillin, and 100 μg/mL streptomycin [38]. Bone marrow-derived macrophages (BMM) were obtained by treating bone marrow cells with macrophage colony-stimulating factor (M-CSF). Briefly, mice were sacrificed, bone marrow was isolated from the hind legs. The bones were flushed with RPMI 1640 medium using a 5-mL syringe and a 25-gauge needle. Bone marrow cells were isolated and cultured in complete RPMI 1640 media containing recombinant murine M-CSF (10 ng/mL, Peprotech, Rocky Hill, NJ, USA) for 5–7 days [43,44].

2.9. Human macrophage culture

Human peripheral blood monocytes were isolated from each subject by density gradient centrifugation and cultured as our described previously [45]. Briefly, human peripheral blood monocytes were differentiated into macrophages using human macrophage colony stimulating factor (M-CSF, 1 ng/mL, Peprotech, Rocky Hill, NJ, USA) for 5 days. The investigation conforms to the principles outlined in the Declaration of Helsinki. The study protocol was approved by the ethics committees of Nanjing Medical University. Written informed consent was obtained from all volunteers.

2.10. Statistical analysis

All data are presented as means ± s.e.m. as indicated. Statistical analysis was performed by a two-tailed unpaired Student's *t*-test or one-way ANOVA (analysis of variance), followed by the post hoc Tukey's test. For all tests, *P*-values lower than 0.05 were considered statistically significant.

3. Results

3.1. Effects of H_2S on NLRP3 inflammasome activation of macrophages exposed to H_2O_2

IL-1β, which is synthesized mainly by monocytes and macrophages, is a powerful mediator of inflammatory response to sterile insults. The stimulation of H_2O_2 on macrophages cells induced the transcription of proinflammatory mediators [46]. To determine whether H_2O_2 induces NLRP3-mediated IL-1β production in macrophages, we ascertained NLRP3-inflammasome activation of macrophages exposed to H_2O_2. The IL-1β production and caspase-1 activation were analyzed by western blotting and we found that macrophages (human primary macrophages and THP-1-derived macrophages) responded to H_2O_2 with a significant increasing of IL-1β production and caspase-1 activation (Fig. 1A and Supplementary Fig. 1A). However, IL-1β production and caspase-1 activation were reduced by pretreatment of macrophages with NaHS (H_2S donor; Fig. 1A and Supplementary Fig. 1A). Next, we measured the co-localization of caspase-1 and NLRP3 in the presence or absence of H_2S. Findings showed an increased co-localization of caspase-1 and NLRP3 in macrophages (human primary macrophages and THP-1-derived macrophages) exposed to H_2O_2, while the effect was again rescued by H_2S (Fig. 1B and Supplementary Fig. 1B). Moreover, the protein levels of H_2S-producing enzymes CBS, CSE, and 3-MST were measured and findings showed that the expression of H_2S-producing enzymes were decreased in H_2O_2-treated macrophages (Supplementary Fig. 1C). The decreased IL-1β production and caspase-1 activation in H_2S-pretreated macrophages might be dependent on NLRP3 inflammasome activation. To test this hypothesis, the NLRP3 was knocked down in THP-1-derived macrophages by short interfering RNA (siRNA, Supplementary Fig. 1D). Results showed that IL-1β production and caspase-1 activation from the THP-1-derived macrophages with NLRP3 knockdown was substantially diminished in response to H_2O_2 with or without H_2S pretreatment (Supplementary Fig. 1E). Recent studies have indicated that oxidative stress-induced mtROS generation leads to NLRP3 inflammasome formation and activation in macrophages [47]. Thus, THP-1-derived macrophages were pretreated with the $P2X_7$ antagonists A438079, cathepsin B inhibitor CA-074Me, or Mito-TEMPO prior to stimulation with H_2O_2. Surprisingly, when macrophages were pretreated with Mito-TEMPO, but not with A438079 or CA-074Me, we observed decreased IL-1β production and caspase-1 activation in macrophages exposed to H_2O_2 (Supplementary Fig. 2A). Therefore, H_2O_2-induced NLRP3 inflammasome activation was independent of $P2X_7$ receptor, or the cathepsin B activation, but dependent on the mitochondrial ROS generation in macrophages.

3.2. Effects of H_2S on mitochondrial ROS production of macrophages exposed to H_2O_2

To determine whether the protective role of H_2S against NLRP3 inflammsome activation is related to reduction of mitochondrial ROS (mtROS), mitochondrial redox status was monitored by the mitochondrial superoxide-sensitive dye MitoSOX. The fluoroprobe MitoSOX was introduced for selective detection of superoxide in the mitochondria of live cells and was validated with confocal microscopy by measuring the

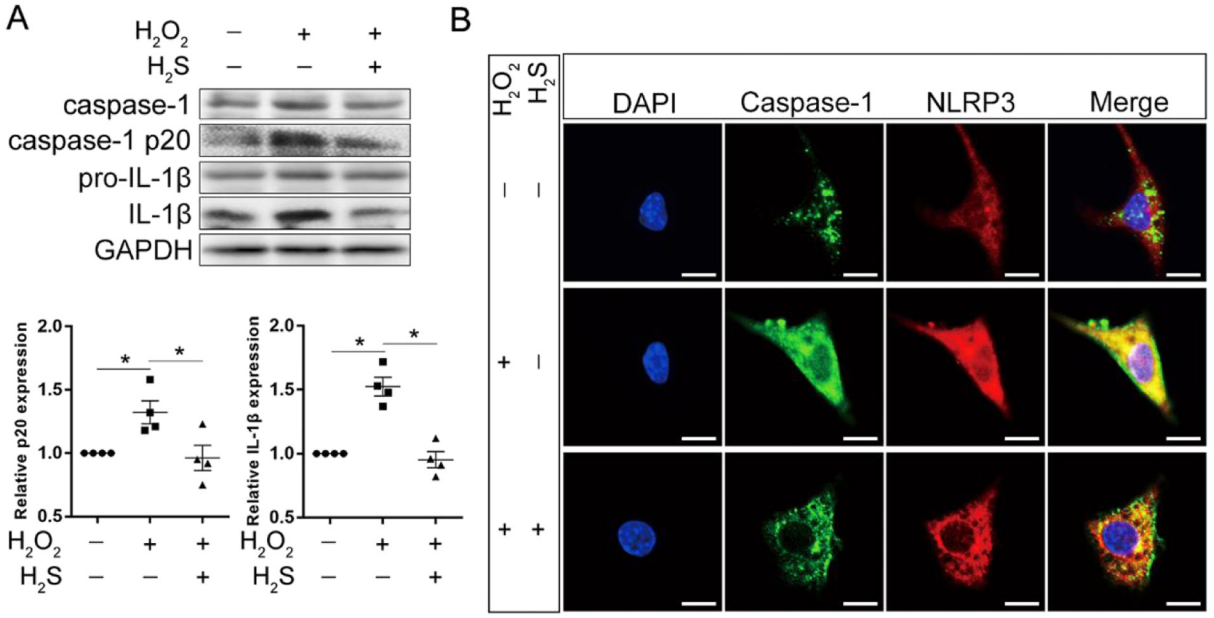

Fig. 1. Protective effects of H_2S on H_2O_2-induced NLRP3 inflammasome activation in macrophages. **(A)** and **(B)** Human primary macrophages were pretreated with NaHS (100 μM; H_2S donor) for 4 h before H_2O_2 (250 μM) for a further 4 h. **(A)** Representative western blotting and quantification of caspase-1, caspase-1 p20, pro-IL-1β, and IL-1β protein expression. Data are means ± s.e.m., $n = 4$, $^*P < 0.05$ (one-way ANOVA, post hoc Tukey). **(B)** Intracellular co-localization of caspase-1 and NLRP3 in the presence and absence of H2S was examined by confocal microscopy. Representative data were shown from three independent experiments ($n = 3$). Scale bars, 10 μm.

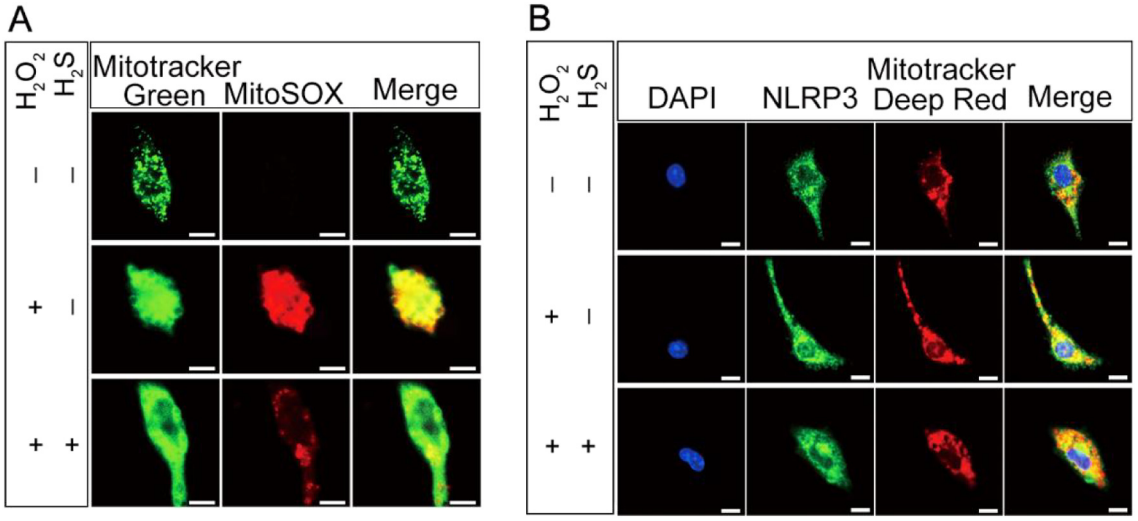

Fig. 2. Effects of H_2S on cellular ROS and mitochondrial ROS production of macrophages exposed to H_2O_2. Human primary macrophages were pretreated with NaHS (100 μM; H_2S donor) for 4 h before H_2O_2 (250 μM) for a further 4 h. **(A)** Mitochondrial ROS was measured using MitoSOX. Mitochondrial localization of MitoSOX signal was confirmed by co-localization with MitoTracker Green. Representative data were shown from three independent experiments (n = 3). Scale bars, 10 μm. **(B)** Mitochondrial recruitment of NLRP3 was examined by using MitoTracker Deep Red stain and multicolor confocal immunofluorescence microscopy. Representative data were shown from three independent experiments (n = 3). Scale bars, 10 μm.

mtROS. MitoSOX fluorescence colocalized with the mitochondria as detected using the probe MitoTracker Green. As expected, treatment of macrophages (human primary macrophages and THP-1-derived macrophages) with H_2O_2 resulted in mtROS generation as demonstrated by an increasing in MitoSOX fluorescence; however, pretreatment with H_2S attenuated mtROS generation (Fig. 2A and Supplementary Fig. 2A). Moreover, recruitment of NLRP3 to mitochondrial was detected with MitoTracker Deep Red stain and multicolor confocal immunofluorescence microscopy. The results exhibited an increased recruitment of NLRP3 by mitochondrial in macrophages (human primary macrophages and THP-1-derived macrophages) exposed to H_2O_2, while the effect was also rescued by H_2S (Fig. 2B and Supplementary Fig. 2B). Furthermore, cellular redox status was monitored by the superoxide-sensitive dye dihydroethidium (DHE). THP-1-derived macrophages responded to H_2O_2 with a significant rise in cellular ROS formation and this rise was reduced by pretreatment of cells with H_2S donor (Supplementary Fig. 2C).

3.3. H_2S S-sulfhydrated c-Jun at cysteine-269 and reduced mtROS production

Previous studies have manifested that H_2S increases activator protein 1 (AP-1) binding activity with SIRT3 promoter and SIRT3 suppresses NLRP3 inflammasome activation in association with decreased

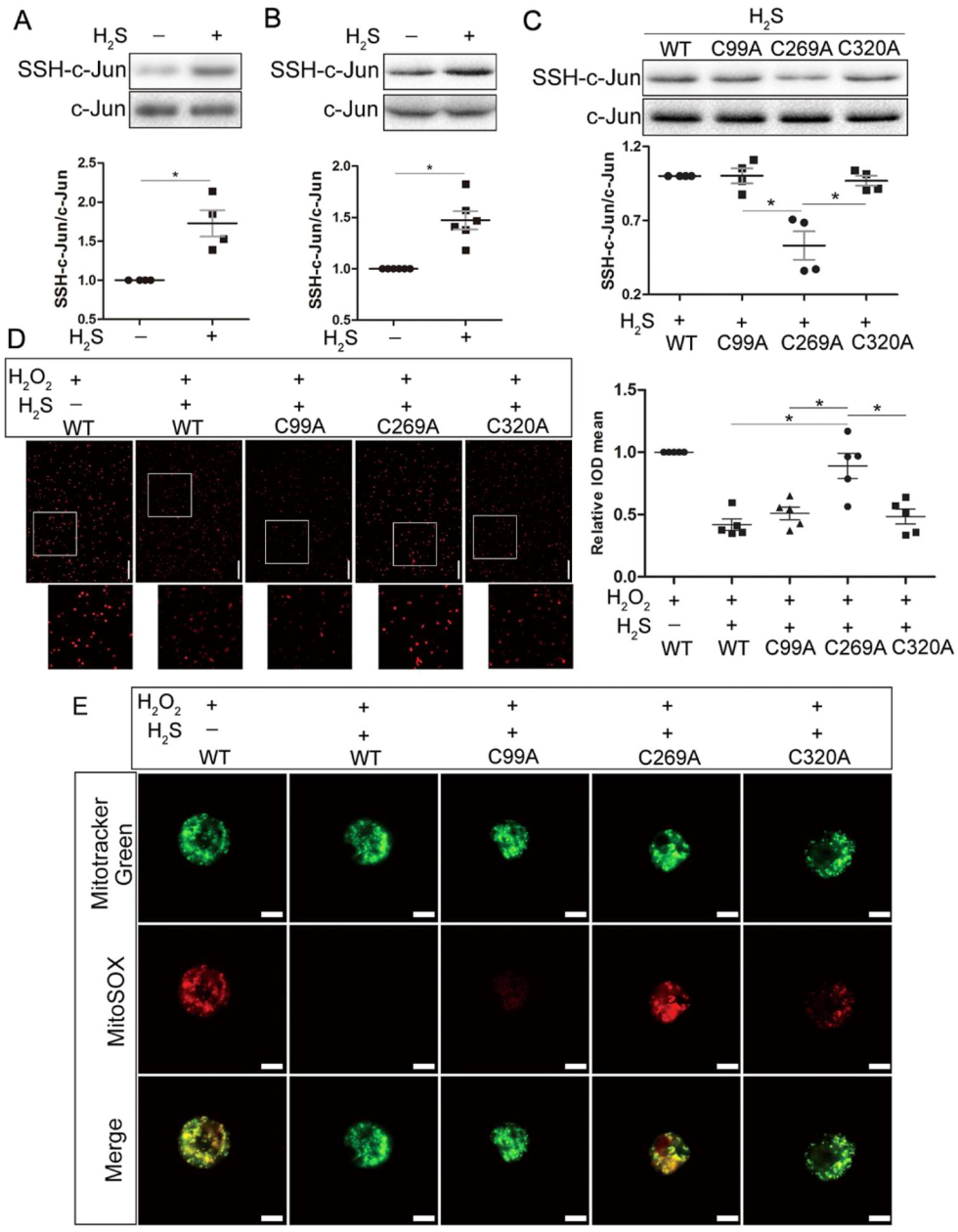

Fig. 3. H_2S S-sulfhydrated the c-Jun at cysteine-269 and reduced mtROS production. **(A)** Human primary macrophages were pretreated with NaHS (100 μM; H_2S donor) for 4 h. After that, the cells were collected for modified biotin switch assay and western blotting for c-Jun. Representative western blotting and quantification of S-sulfhydrated c-Jun and c-Jun protein expression. Data are means ± s.e.m., $n = 4$, $^*P < 0.05$ (two-tailed unpaired Student's *t*-test). **(B)** THP-1-derived macrophages were transfected with control or wild-type c-Jun plasmids for 24 h 4 following incubation of NaHS (100 μM) for additional 4 h. After that, the cells were collected for modified biotin switch assay and western blotting for c-Jun. Representative western blotting and quantification of S-sulfhydrated c-Jun and c-Jun protein expression. Data are means ± s.e.m., $n = 6$, $^*P < 0.05$ (two-tailed unpaired student's *t*-test). **(C)** THP-1-derived macrophages were transfected with control or wild-type c-Jun plasmids or wild-type c-Jun, C99A mutant, C269A mutant, and C320A mutant plasmids for 24 h following incubation of NaHS (100 μM) for additional 4 h. Representative western blotting and quantification of S-sulfhydrated c-Jun and c-Jun protein expression. Data are means ± s.e.m., n = 4, $^*P < 0.05$ (one-way ANOVA, post hoc Tukey). **(D)** and **(E)** THP-1-derived macrophages were transfected with wild-type c-Jun, C99A mutant, C269A mutant, and C320A mutant plasmids for 24 h following incubation of NaHS (100 μM) for additional 4 h before H_2O_2 (250 μM) for a further 4 h. **(D)** Cellular ROS production was detected by DHE staining. Scale bars, 100 μm. Data are means ± s.e.m., $n = 5$, $^*P < 0.05$ (one-way ANOVA, post hoc Tukey). **(E)** Mitochondrial ROS was measured using fluorescent probe MitoSOX. Mitochondrial localization of MitoSOX signal was confirmed by co-localization with MitoTracker Green. Representative data were shown from three independent experiments ($n = 3$). Scale bars, 10 μm.

mtROS production. We wondered whether H_2S mediates the decreased mtROS production by S-sulfhydrating c-Jun (subunit of AP-1) in macrophages. S-sulfhydration is a physiological process wherein H_2S attaches an additional sulfur to the thiol (–SH) groups of cysteines yielding a hydropersulfide (–SSH). We examined S-sulfhydration of c-Jun in macrophages exposed to H_2S by the modified biotin switch assay. As expected, S-sulfhydration of c-Jun in macrophages (human primary macrophages and THP-1-derived macrophages) markedly increased after H_2S treatment (Fig. 3A and Fig. 3B). To identify the S-sulfhydrated cysteine residue of c-Jun, we mutated cysteine-99, cysteine-269, and cysteine-320 (the only three cysteine residues) in the c-Jun protein. All the mutants contained only a single amino acid mutation (cysteine to alanine) at the designated residue (C99A, C269A, C320A). Mutation of cysteine-269, but not cysteine-99 and cysteine-320 abolished the increased level of c-Jun S-sulfhydration after H_2S treatment compared with wild-type c-Jun transfection (Fig. 3C and Supplementary Fig. 3). To determine whether C269 was involved in H_2S-reduced mtROS production, DHE and MitoSOX Red assays were performed. We found that THP-1-derived macrophages responded to H_2O_2 with a significant rise in cellular ROS and mtROS formation, which was rescued by H_2S treatment (Fig. 3D and E). However, mutation of C269, but not C99 or C320 in the c-Jun protein, reversed the effects of H_2S on the reducing of cellular ROS and mtROS production, pointing to the critical role of C269 in c-Jun S-sulfhydration. (Fig. 3D and E).

3.4. Effects of S-sulfhydrated c-Jun on NLRP3 inflammasome activation

Since S-sulfhydrated c-Jun reduced mtROS production, we examined the influences of S-sulfhydrated c-Jun on NLRP3 inflammasome activation. We transfected the wild-type c-Jun or C269A plasmids to THP-1-derived macrophages exposed to H_2O_2. Results showed that S-sulfhydration of c-Jun increased by pretreatment with H_2S in wild-type c-Jun-transfected macrophages, while mutation of C269 in the c-Jun protein reversed the effect of H_2S on c-Jun S-sulfhydration (Fig. 4A). Furthermore, IL-1β production and caspase-1 activation were reduced by pretreatment of wild-type c-Jun-transfected macrophages with H_2S, while these influences of S-sulfhydrated c-Jun were also reversed in C269A-transfected macrophages (Fig. 4B). Additionally, we measured

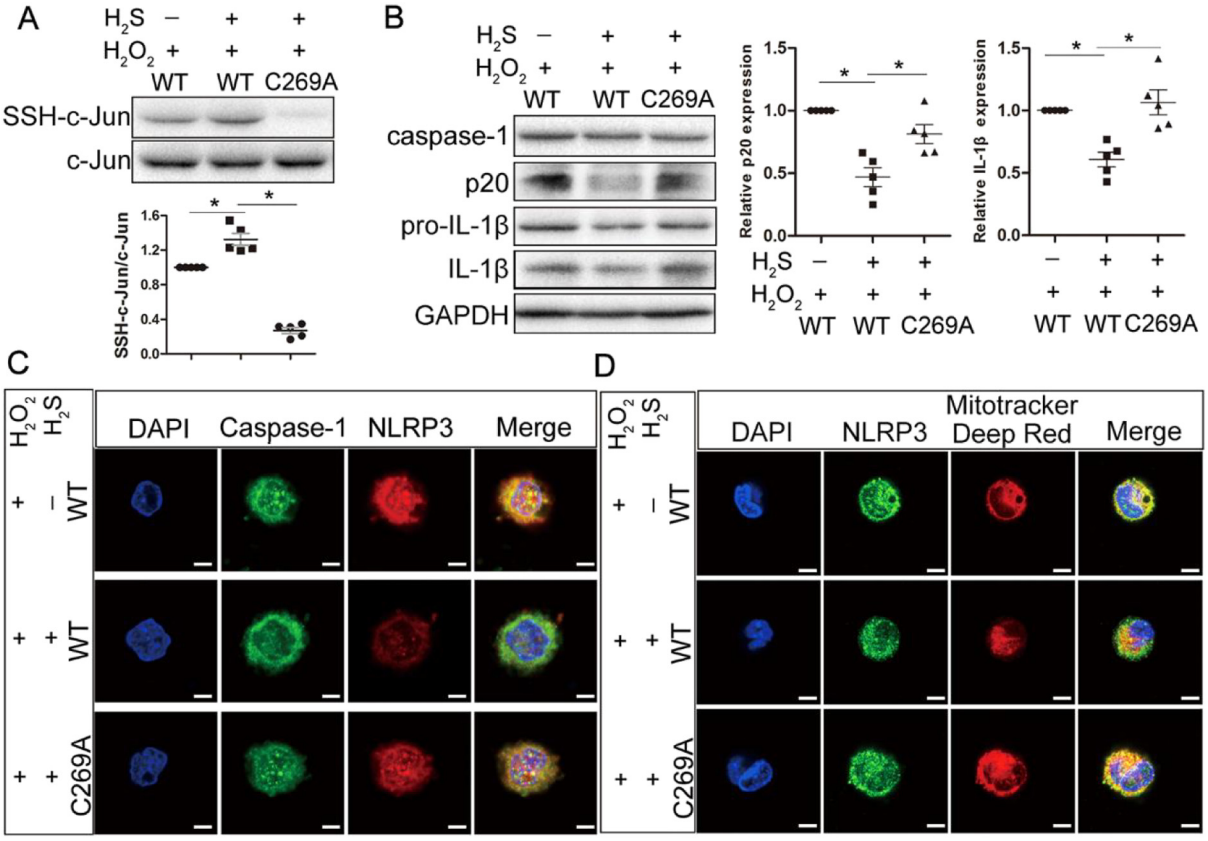

Fig. 4. Effects of S-sulfhydrated c-Jun on NLRP3 inflammasome activation. THP-1-derived macrophages were transfected with wild-type c-Jun and C269A mutant plasmids for 24 h. After that macrophages were treated the same as described in Fig. 1. **(A)** Cells were collected for modified biotin switch assay and western blotting for c-Jun. Representative western blotting and quantification of S-sulfhydrated c-Jun and c-Jun protein expression. Data are means ± s.e.m., n = 5, $^*P < 0.05$ (one-way ANOVA, post hoc Tukey). **(B)** Representative western blotting and quantification of caspase-1, caspase-1 p20, pro-IL-1β, and IL-1β protein expression. Data are means ± s.e.m., n = 5, $^*P < 0.05$ (one-way ANOVA, post hoc Tukey). **(C)** Intracellular co-localization of caspase-1 and NLRP3 in the presence and absence of H_2S was examined by confocal microscopy. Representative data were shown from three independent experiments (n = 3). Scale bars, 10 μm. **(D)** Mitochondrial recruitment of NLRP3 was examined by using MitoTracker Deep Red stain and multicolor confocal immunofluorescence microscopy. Representative data were shown from three independent experiments (n = 3). Scale bars, 10 μm.

the co-localization of caspase-1 and NLRP3 in the wild-type c-Jun- or C269A-transfected THP-1-derived macrophages. As expected, pretreatment with H_2S showed an attenuated co-localization of caspase-1 and NLRP3 in wild-type c-Jun-transfected macrophages, while this effect of S-sulfhydrated c-Jun was again reversed in C269A-transfected macrophages (Fig. 4C). Similarly, co-localization of NLRP3 with mitochondria was also decreased in wild-type c-Jun-transfected group and increased in C269A-transfected group (Fig. 4D). Collectively, these results suggested that H_2S inhibited the NLRP3 inflammasome activation via S-sulfhydration of c-Jun at cysteine-269.

3.5. S-sulfhydration of c-Jun enhanced its transcriptional activity on SIRT3 and p62

Previous studies have revealed that SIRT3 and p62 suppress NLRP3 inflammasome activation in association with mtROS production and damaged mitochondria clearance, respectively. Additionally, c-Jun is an important factor in p62 transcription. As expected, treatment of human primary macrophages with H_2O_2 decreased the expression of SIRT3 and p62; however, pretreatment with H_2S restored the SIRT3 and p62 expression (Fig. 5A). To test whether the upregulated expression of SIRT3 and p62 induced by H_2S is independent on its direct mtROS-scavenging effect, we treated macrophages with the mitochondria-targeted antioxidant Mito-TEMPO prior to exposure to H_2O_2 and measured the expression of SIRT3 and p62. However, results showed that the pretreatment of Mito-TEMPO failed to increase the levels of SIRT3 and p62 (Supplementary Fig. 4). Furthermore, we transfected the wild-type c-Jun or C269A plasmids to THP-1-derived macrophages exposed to H_2O_2 and explored the nuclear translocation of c-Jun in the wild-type c-Jun- or C269A-transfected macrophages. The results showed that pretreatment with H_2S displayed an increased nuclear translocation of c-Jun in wild-type c-Jun-transfected macrophages, while this effect of S-sulfhydrated c-Jun was again reversed in C269A-transfected macrophages (Fig. 5B). To investigate whether S-sulfhydrated c-Jun could increase SIRT3 and p62 expression, we examined the expression of SIRT3 and p62 by using real-time PCR and western blotting assays. Findings showed that the mRNA levels of SIRT3 and p62 increased by pretreatment with H_2S in wild-type c-Jun-transfected macrophages, while this effect of S-sulfhydrated c-Jun was reversed in C269A-transfected macrophages (Fig. 5C). Consistently, the protein levels of SIRT3 and p62 also increased by pretreatment with H_2S in wild-type c-Jun-transfected macrophages, while this influence of S-sulfhydrated c-Jun was again reversed in C269A-transfected macrophages (Fig. 5D). To investigate whether the S-sulfhydration of c-Jun could regulate its transcriptional activation, pAP1-TA-luc luciferase reporter plasmids, a vector construct with multiple c-Jun/AP-1 (TGACTAA) response elements, was transfected into macrophages. The reporter assays revealed a reduced luciferase activity in macrophages exposed to H_2O_2; however, the activity was reversed by H_2S (Fig. 5E). Furthermore, we found that the promoters (−500−−1) of human SIRT3 (−337−−325) and p62 (−389−−377) contain c-Jun response element by using JASPAR databases (http://jaspar.genereg.net/) (Supplementary data 1). A

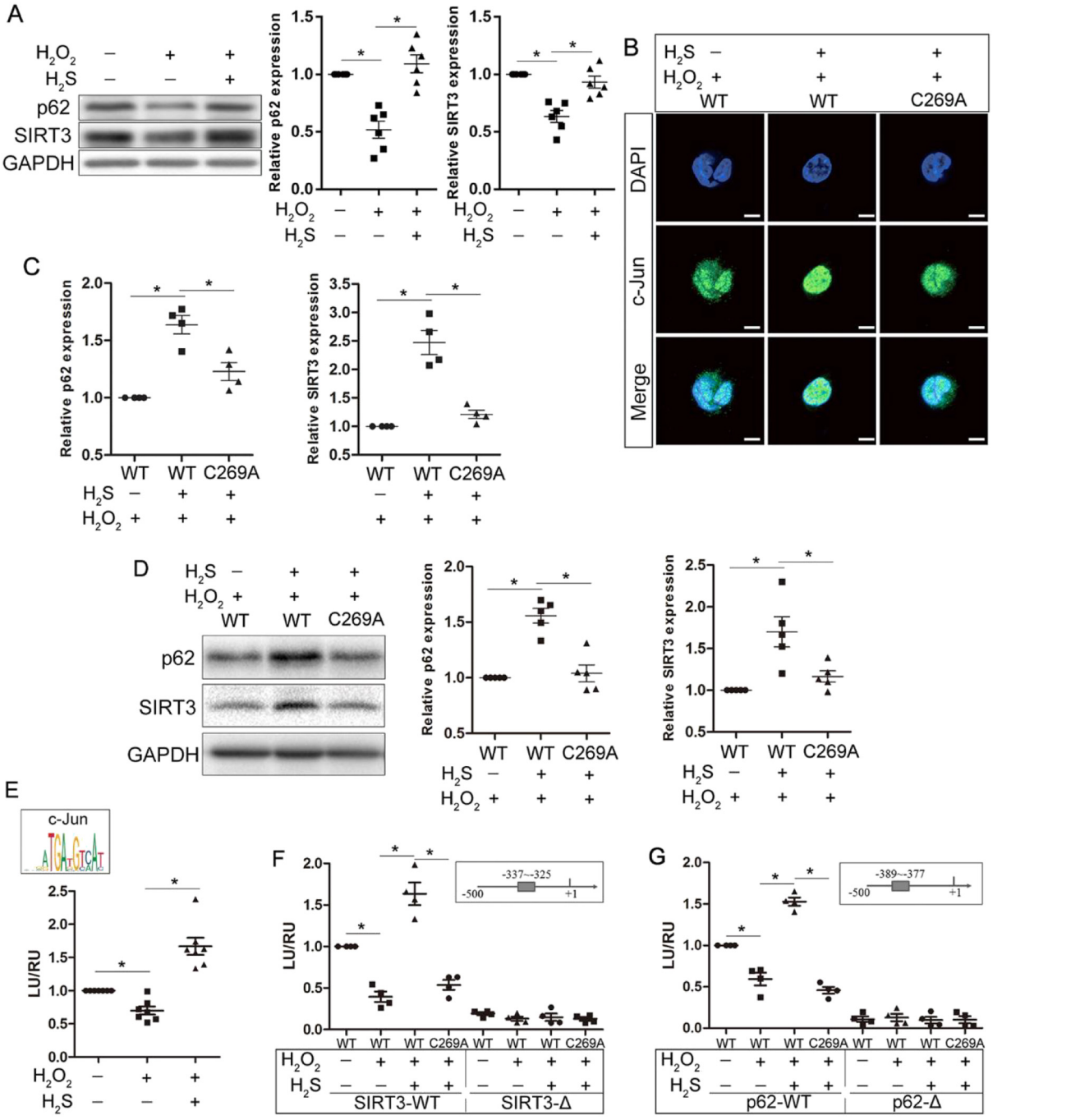

Fig. 5. S-sulfhydration of c-Jun enhanced its transcriptional activity on SIRT3 and p62. **(A)** Human primary macrophages were pretreated with NaHS (100 μM; H2S donor) for 4 h before H_2O_2 (250 μM) for a further 4 h. Representative western blotting and quantification of SIRT3 and p62 protein expression. Data are means ± s.e.m., n = 6, $^*P < 0.05$ (one-way ANOVA, post hoc Tukey). **(B-G)** THP-1-derived macrophages were treated the same as described in Fig. 4. **(B)** Intracellular distribution of c-Jun was determined by confocal microscopy. Representative data were shown from three independent experiments (n = 3). Scale bars, 10 μm. **(C)** The expression SIRT3 and p62 of mRNA was determined by real-time PCR. Data are means ± s.e.m., n = 4, $^*P < 0.05$ (one-way 7 ANOVA, post hoc Tukey). **(D)** Representative western blotting and quantification of SIRT3 and p62 protein expression. Data are means ± s.e.m., n = 5, $^*P < 0.05$ (one-way ANOVA, post hoc Tukey). **(E)** Macrophages were transfected with pAP1-TA-luc luciferase vector and pGL4.74 plasmids for 12 h following incubation of NaHS (100 μM) for additional 4 h before H2O2 (250 μM) for a further 4 h. The luciferase activity was determined using a dual-luciferase reporter assay system. Data are means ± s.e.m., $n = 7$, $^*P < 0.05$ (one-way ANOVA, post hoc Tukey). **(F)** Macrophages were transfected with wild-type c-Jun or C269A mutant plasmids. After 24 h cells were transfected with SIRT3-WT or SIRT3-Δ (p62-WT or p62-Δ **(G)**) luciferase vector and pGL4.74 plasmids for 12 h following incubation of NaHS (100 μM) for additional 4 h before H_2O_2 (250 μM) for a further 4 h. The luciferase activity was determined using a dual-luciferase reporter assay system. Data are means ± s.e.m., n = 4, $^*P < 0.05$ (one-way ANOVA, post hoc Tukey).

number of luciferase reporter plasmids containing the wild type and deletion of the c-Jun response elements in the SIRT3 and p62 promoter were constructed. With the deletion constructs, the stimulatory effects of H_2S on SIRT3 or p62 promoter activity were observed in c-Jun-wild type and SIRT3-WT or p62-WT transfected THP-1-derived macrophages. However, H_2S-induced enhancement of SIRT3 or p62 promoter activity was abolished in c-Jun-C269A and SIRT3-Δ or p62-Δ transfected macrophages (Fig. 5F and G). These suggest that the c-Jun

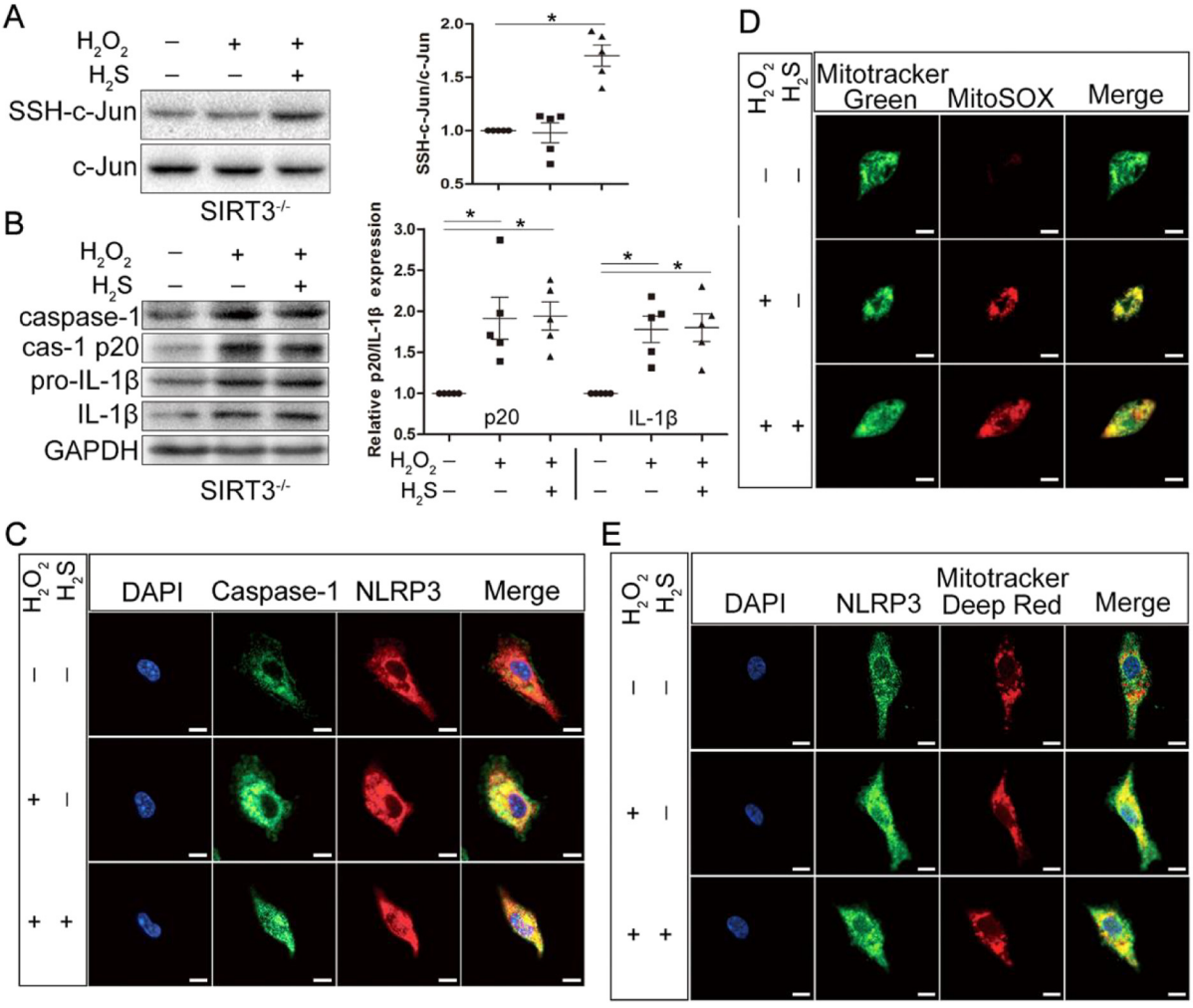

Fig. 6. The protective effects of H2S on SIRT3$^{-/-}$ mice macrophage. Peritoneal macrophages and bone marrow-derived macrophages (BMM) were treated the same as described in Fig. 1. **(A)** SIRT3$^{-/-}$ bone marrow-derived macrophages were collected for modified biotin switch assay and western blotting for c-Jun. Representative western blotting and quantification of S-sulfhydrated c-Jun and c-Jun protein expression. Data are means ± s.e.m., n = 5, $^{*}P < 0.05$ (one-way ANOVA, post hoc Tukey). **(B)** Representative western blotting and quantification of caspase-1, caspase-1 p20, pro-IL-1β, and IL-1β protein expression in SIRT3$^{-/-}$ BMM. Data are means ± s.e.m., n = 5, $^{*}P < 0.05$ (one-way ANOVA, post hoc Tukey). **(C)** Intracellular co-localization of caspase-1 and NLRP3 in the presence and absence of H_2S was examined by confocal microscopy in SIRT3$^{-/-}$ peritoneal macrophages. Representative data were shown from three independent experiments (n = 3). Scale bars, 10 μm. **(D)** Mitochondrial localization of MitoSOX signal was confirmed by co-localization with MitoTracker Green in SIRT3peritoneal macrophages. Representative data were shown from three independent experiments (n = 3). Scale bars, 10 μm. **(E)** Mitochondrial recruitment of NLRP3 9 was examined by using MitoTracker Deep Red stain and multicolor confocal immunofluorescence microscopy in SIRT3$^{-/-}$ peritoneal macrophages. Representative data were shown from three independent experiments (n = 3). Scale bars, 10 μm.

response elements on the upstream of the SIRT3 and p62 promoters are responsible for the effects of H_2S on SIRT3 and p62 transcription by S-sulfhydrating c-Jun. Collectively, these results suggest that H_2S upregulates the SIRT3 and p62 genes expression via S-sulfhydrating c-Jun and increasing its binding activity with the SIRT3 and p62 promoters.

3.6. The protective effects of H_2S on macrophage from SIRT3$^{-/-}$ mice

Our results suggest that H_2S-regulated SIRT3 plays an important role in the regulation of oxidative stress and inflammation response through S-sulfhydrating c-Jun in macrophages exposed to H_2O_2 in vitro. To further confirm the pathophysiological significance of H_2S-induced SIRT3 expression, we examined the protective effects of H_2S on mtROS generation and NLRP3 inflammasome activation in SIRT3$^{-/-}$ mice macrophages. Peritoneal macrophages and bone marrow-derived macrophages (BMM) were pretreated with H_2S before H_2O_2 treatment. Firstly, we confirmed that S-sulfhydration of c-Jun still increased by pretreatment with H_2S in SIRT3$^{-/-}$ BMM (Fig. 6A). Secondly, however, the activation of caspase-1 and production of IL-1β did not reduce in SIRT3$^{-/-}$ BMM exposed to H_2O_2 and H_2S pretreatment (Fig. 6B). Thirdly, the increasing of co-localization of caspase-1 and NLRP3 in SIRT3$^{-/-}$ peritoneal macrophages exposed to H_2O_2 also did not rescue with H_2S pretreatment (Fig. 6C). Fourthly, treatment of SIRT3$^{-/-}$ peritoneal macrophages with H_2O_2 resulted in mtROS generation and pretreatment with H_2S also did not attenuate this effect (Fig. 6D). Fifthly, the recruitment of NLRP3 to mitochondrial also displayed no difference in SIRT3$^{-/-}$ peritoneal macrophages exposed to H_2O_2 in the presence and absence of H_2S (Fig. 6E). These results demonstrated that SIRT3 was required for H_2S to inhibit excessive oxidative stress and NLRP3 inflammasome activation in macrophages.

4. Discussion

Cardiovascular risk factors such as hypercholesterolemia, hypertension, and diabetes mellitus enhance ROS generation, resulting in oxidative stress [48]. Macrophage, the dominant cell type recruited to

inflammatory sites, is known to secrete ROS and may be primarily responsible for oxidative damage. Numerous stimuli such as oxidized low-density lipoprotein (OxLDL), high glucose, hydrogen peroxide (H_2O_2), tumor necrosis factor (TNF), and hypoxia can cause oxidative stress and promote macrophage inflammation, which is associated with the pathophysiology of cardiovascular diseases [49–54]. The reactive oxygen species that are generated by mitochondrial respiration, especially H_2O_2, are potent inducers of oxidative damage [55]. Here, we treated macrophages with exogenous H_2O_2 for mimicking different stimuli-induced oxidative stress in macrophages. Remarkably, H_2O_2-treated macrophages showed an increase in oxidative stress and inflammation [46,52,56,57]. In the present study, we demonstrated that H_2O_2 could induce the activation of NLRP3 inflammasome, leading to the activation of caspase-1 and production of pro-inflammatory cytokines IL-1β in macrophages. Moreover, as evident from the NLRP3 siRNA studies, we demonstrated that H_2O_2-induced IL-1β production and caspase-1 activation was dependent on NLRP3 inflammasome activation. We also found that the expression of H_2S-producing enzymes was decreased in H_2O_2-treated macrophages, indicating the generation of endogenous H_2S was decreased. In consideration of the powerful antioxidative and anti-inflammatory properties of H_2S, we next put our focus on whether H_2S could play a protective role in reducing oxidative stress and inflammation in macrophages exposed to H_2O_2. Similarly, our data showed that exogenous H_2S treatment protected macrophages from NLRP3 inflamasome activation against H_2O_2 insult. Recent studies suggest that H_2S reduces NLRP3 inflammasome activation in free fatty acids and monosodium urate (MSU) crystals-stimulated macrophages, or microglia after intracerebral haemorrhage [58–60]. What we observed in macrophages stimulated with H_2O_2 is that oxidative stress-induced NLRP3 inflammasome activation is dependent on the mitochondrial ROS generation, but not $P2X_7$ receptor or cathepsin B activation. These results are consistent with the study of Castelblanco et al., which showed that H_2S donors inhibited MSU crystal-induced mtROS generation [60]. It remains to be further elucidated whether the protective role of H_2S against NLRP3 inflammsome activation is related to mtROS reduction, as the conception that mtROS induces NLRP3-dependent inflammasome activation has been established [61,62]. For example, mitochondrial oxidative stress in lesional macrophages amplifies atherosclerotic lesion development by promoting NF-κB-mediated entry of monocytes and other inflammatory processes [63]. Additionally, NLRP3 inflammasome activation by mitochondrial oxidative stress in macrophages contributes to the development of angiotensin II–induced aortic aneurysm [64]. Interestedly, we observed that generation of mtROS and recruitment of NLRP3 to mitochondrial was increased in macrophages exposed to H_2O_2, while these effects of H_2O_2 was rescued by H_2S treatment. Therefore, for the first time, we demonstrated that H_2S protected macrophages from H_2O_2-induced NLRP3 inflammasome activation via reducing the generation of mtROS.

Our next focus is to explore how H_2S reduced the generation of mtROS. H_2S can cause protein S-sulfhydration (or persulfidation) to affect their functions [29,65]. Previous studies have demonstrated that S-sulfhydration of GAPDH affects PSD95 degradation and memory [66]. And S-sulfhydration of NF-κB inhibits apoptosis [67]. S-sulfhydration of K_{ATP} could contribute to H_2S-induced vasodilation [68]. H_2S is also involved in endoplasmic reticulum stress via triggering S-sulfhydration of PTP1B [69]. In recent years, more and more proteins have been found to be regulated by S-sulfhydration [65]. Our groups have previously characterized that H_2S increases AP-1 binding activity with SIRT3 promoter, thus enhancing SIRT3 transcription to attenuate endothelial oxidative stress [37]. Accordingly, we wondered whether H_2S could S-sulfhydrated c-Jun (subunit of AP-1) in macrophages. Interestingly, we found that c-Jun is basically S-sulfhydrated and exogenously applied H_2S further enhanced c-Jun S-sulfhydration. To discover S-sulfhydrated cysteine residues of c-Jun, we mutated cysteine-99, cysteine-269, and cysteine-320 (the only three cysteine residues) in c-Jun protein. We confirmed that cysteine-269 was responsible for c-Jun S-sulfhydration. However, mutation of cysteine-269, but not cysteine-99 and cysteine-320, largely prevented the protective influences of H_2S on the reducing of ROS and mtROS production exposed to H_2S, pointing to the critical role of C269 in c-Jun S-sulfhydration. After that, we explored the effects of S-sulfhydrated c-Jun on NLRP3 inflammasome activation. As expected, the results showed that S-sulfhydration of c-Jun cysteine-269 was involved in suppressing NLRP3 inflammasome activation by H_2S in macrophages exposed to H_2O_2. Therefore, we demonstrated that the H_2S inhibited the NLRP3 inflammasome activation via S-sulfhydration c-Jun at cysteine-269. Taken together, the findings that mutation of the c-Jun S-sulfhydrated cysteines diminished the suppressive influences of H_2S on NLRP3 inflammasome activation are consistent with the suggestion that there is a relevant link between the S-sulfhydration of c-Jun and its antioxidative properties by H_2S.

SIRT3 can enhance antioxidant enzyme activity to exert its ROS-scavenging capacity [37,70]. Recent studies have shown that SIRT3 decreases NLRP3 inflammasome activation in association with diminished mtROS production via activating SOD2 [71,72]. Several groups, including our own, have previously indicated that c-Jun/AP-1 is able to bind with SIRT3 promoter and enhances its expression [37,73,74]. p62 binds polyubiquitinated proteins and damaged organelles and targets them to autophagosomal clearance via its ubiquitin association domain and LC3 binding motif, respectively [75,76]. Additionally, p62 also has antioxidant capacity [77–80]. p62 is recruited to damaged mitochondria and eliminates them, thus contributing to the prevention of excessive inflammasome activation [76]. Moreover, c-Jun/AP-1 is an important factor in p62 transcription [81–83]. The question we posed here is whether S-sulfhydrated c-Jun could increase SIRT3 and p62 expression. The findings in this study showed that, via a c-Jun C269-dependent manner, the S-sulfhydrated c-Jun resulted in increasing SIRT3 and p62 expression and protected macrophages against H_2O_2 insult. To further confirm that the upregulated expression of SIRT3 and p62 induced by H_2S is independent on its direct mtROS-scavenging effect, we treated macrophages with the mitochondria-targeted antioxidant Mito-TEMPO prior to exposure to H_2O_2 and found that the pretreatment of Mito-TEMPO failed to increase the levels of SIRT3 and p62. These results suggested the antioxidant effects of H_2S were mainly dependent on S-sulfhydrated c-Jun in H_2O_2-treated macrophages. However, both mRNA and protein expression of SIRT3 was significantly enhanced by H_2S in H_2O_2-exposed macrophages. This phenomenon drove us to focus on SIRT3. Moreover, we found that the influences of H_2S on mtROS generation and NLRP3 inflammasome activation was diminished in the macrophages of $SIRT3^{-/-}$ mice, suggesting that the protective effects of H_2S against oxidative stress and NLRP3 inflammasome activation partly dependent on SIRT3.

Taken together, the results showed that H_2S is privotal in the regulation of oxidative stress and inflammation response through S-sulfhydrating c-Jun in macrophages exposed to H_2O_2 (Fig. 7). H_2S donors have therapeutic potential for diseases such as cancer, peptic ulcer

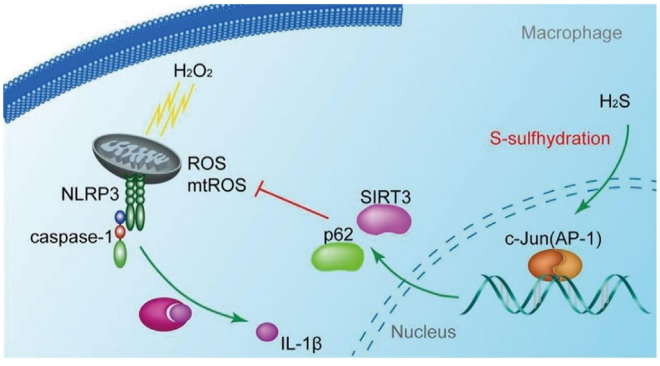

Fig. 7. The proposed signaling pathway underlying H2S regulation of c-Jun by S-sulfhydration in macrophages.

disease, acute and chronic inflammatory diseases, Parkinson's and Alzheimer's disease and erectile dysfunction, arterial and pulmonary hypertension, atherosclerosis, heart failure [84,85]. H_2S is also regulated by many currently used drugs, such as statins, aspirin, and metformin, but the mechanism of these effects and their clinical implications are only started to be understood [85]. Our findings provide a specific molecular mechanism for therapeutic potential of H_2S donors in cardiovascular disease. Modifications of c-Jun may offer promise in the therapy of cardiovascular disease. Therefore, H_2S donors selectively targeted to c-Jun may provide notable benefit.

Conflict of interest

The authors declare that there is no conflict of interest.

Transparency document

The Transparency document associated with this article can be found, in online version.

Acknowledgments

This work was supported by grants from the National Natural Science Foundation of China (grant nos. 91639204, 81330004, 81670209, 81770287, 81200196).

Appendix A. Supplementary data

Supplementary data to this article can be found online at https://doi.org/10.1016/j.bbadis.2018.05.023.

References

[1] S. Bansilal, J.M. Castellano, V. Fuster, Global burden of Cvd: focus on secondary prevention of cardiovascular disease, Int. J. Cardiol. 201 (Suppl 1) (2015) S1–S7.
[2] F. Santilli, M.T. Guagnano, N. Vazzana, S. La Barba, G. Davi, Oxidative stress drivers and modulators in obesity and cardiovascular disease: from biomarkers to therapeutic approach, Curr. Med. Chem. 22 (2015) 582–595.
[3] D.I. Brown, K.K. Griendling, Regulation of signal transduction by reactive oxygen species in the cardiovascular system, Circ. Res. 116 (2015) 531–549.
[4] W.G. Mcmaster, A. Kirabo, M.S. Madhur, D.G. Harrison, Inflammation, immunity, and hypertensive end-organ damage, Circ. Res. 116 (2015) 1022–1033.
[5] H.N. Siti, Y. Kamisah, J. Kamsiah, The role of oxidative stress, antioxidants and vascular inflammation in cardiovascular disease (a review), Vasc. Pharmacol. 71 (2015) 40–56.
[6] G. Csanyi, F.J. Miller Jr., Oxidative stress in cardiovascular disease, Int. J. Mol. Sci. 15 (2014) 6002–6008.
[7] Z. Mallat, Macrophages, Arterioscler. Thromb. Vasc. Biol. 34 (2014) 2509–2519.
[8] W. Sun, Y. Pang, Z. Liu, L. Sun, B. Liu, M. Xu, Y. Dong, J. Feng, C. Jiang, W. Kong, X. Wang, Macrophage inflammasome mediates hyperhomocysteinemia-aggravated abdominal aortic aneurysm, J. Mol. Cell. Cardiol. 81 (2015) 96–106.
[9] K.J. Moore, F.J. Sheedy, E.A. Fisher, Macrophages in atherosclerosis: a dynamic balance, Nat. Rev. Immunol. 13 (2013) 709–721.
[10] S. Colin, G. Chinetti-Gbaguidi, B. Staels, Macrophage phenotypes in atherosclerosis, Immunol. Rev. 262 (2014) 153–166.
[11] J. Endo, M. Sano, Y. Isobe, K. Fukuda, J.X. Kang, H. Arai, M. Arita, 18-Hepe, an N-3 fatty acid metabolite released by macrophages, prevents pressure overload-induced maladaptive cardiac remodeling, J. Exp. Med. 211 (2014) 1673–1687.
[12] Z. Liu, S. Morgan, J. Ren, Q. Wang, D.S. Annis, D.F. Mosher, J. Zhang, C.M. Sorenson, N. Sheibani, B. Liu, Thrombospondin-1 (Tsp1) contributes to the development of vascular inflammation by regulating monocytic cell motility in mouse models of abdominal aortic aneurysm, Circ. Res. 117 (2015) 129–141.
[13] G. Faraco, Y. Sugiyama, D. Lane, L. Garcia-Bonilla, H. Chang, M.M. Santisteban, G. Racchumi, M. Murphy, N. Van Rooijen, J. Anrather, C. Iadecola, Perivascular macrophages mediate the neurovascular and cognitive dysfunction associated with hypertension, J. Clin. Invest. 126 (2016) 4674–4689.
[14] L. Rochette, M. Zeller, Y. Cottin, C. Vergely, Diabetes, oxidative stress and therapeutic strategies, Biochim. Biophys. Acta 1840 (2014) 2709–2729.
[15] G. Sisino, T. Bouckenooghe, S. Aurientis, P. Fontaine, L. Storme, A. Vambergue, Diabetes during pregnancy influences Hofbauer cells, a subtype of placental macrophages, to acquire a pro-inflammatory phenotype, Biochim. Biophys. Acta 1832 (2013) 1959–1968.
[16] B.I. Frohnert, E.K. Long, W.S. Hahn, D.A. Bernlohr, Glutathionylated lipid aldehydes are products of adipocyte oxidative stress and activators of macrophage inflammation, Diabetes 63 (2014) 89–100.
[17] E.I. Elliott, F.S. Sutterwala, Initiation and perpetuation of Nlrp3 inflammasome activation and assembly, Immunol. Rev. 265 (2015) 35–52.
[18] R. Allam, M.N. Darisipudi, K.V. Rupanagudi, J. Lichtnekert, J. Tschopp, H.J. Anders, Cutting edge: cyclic polypeptide and aminoglycoside antibiotics trigger Il-1beta secretion by activating the Nlrp3 inflammasome, J. Immunol. 186 (2011) 2714–2718.
[19] S.S. Iyer, Q. He, J.R. Janczy, E.I. Elliott, Z. Zhong, A.K. Olivier, J.J. Sadler, V. Knepper-Adrian, R. Han, L. Qiao, S.C. Eisenbarth, W.M. Nauseef, S.L. Cassel, F.S. Sutterwala, Mitochondrial Cardiolipin is required for Nlrp3 inflammasome activation, Immunity 39 (2013) 311–323.
[20] R. Zhou, A.S. Yazdi, P. Menu, J. Tschopp, A role for mitochondria in Nlrp3 inflammasome activation, Nature 469 (2011) 221–225.
[21] S.M. Man, T.D. Kanneganti, Regulation of inflammasome activation, Immunol. Rev. 265 (2015) 6–21.
[22] P. Duewell, H. Kono, K.J. Rayner, C.M. Sirois, G. Vladimer, F.G. Bauernfeind, G.S. Abela, L. Franchi, G. Nunez, M. Schnurr, T. Espevik, E. Lien, K.A. Fitzgerald, K.L. Rock, K.J. Moore, S.D. Wright, V. Hornung, E. Latz, Nlrp3 inflammasomes are required for atherogenesis and activated by cholesterol crystals, Nature 464 (2010) 1357–1361.
[23] A. Abderrazak, D. Couchie, D.F. Mahmood, R. Elhage, C. Vindis, M. Laffargue, V. Mateo, B. Buchele, M.R. Ayala, M. El Gaafary, T. Syrovets, M.N. Slimane, B. Friguet, T. Fulop, T. Simmet, K. El Hadri, M. Rouis, Anti-inflammatory and antiatherogenic effects of the Nlrp3 inflammasome inhibitor arglabin in Apoe2.Ki mice fed a high-fat diet, Circulation 131 (2015) 1061–1070.
[24] F.J. Sheedy, A. Grebe, K.J. Rayner, P. Kalantari, B. Ramkhelawon, S.B. Carpenter, C.E. Becker, H.N. Ediriweera, A.E. Mullick, D.T. Golenbock, L.M. Stuart, E. Latz, K.A. Fitzgerald, K.J. Moore, Cd36 coordinates Nlrp3 inflammasome activation by facilitating intracellular nucleation of soluble ligands into particulate ligands in sterile inflammation, Nat. Immunol. 14 (2013) 812–820.
[25] Y. Wang, X. Yan, S. Mi, Z. Li, H. Zhu, X. Sun, B. Zhao, C. Zhao, Y. Zou, K. Hu, X. Ding, A. Sun, J. Ge, Naoxintong attenuates ischaemia/reperfusion injury through inhibiting Nlrp3 inflammasome activation, J. Cell. Mol. Med. 21 (2017) 4–12.
[26] W. Gan, J. Ren, T. Li, S. Lv, C. Li, Z. Liu, M. Yang, The Sgk1 inhibitor Emd638683, prevents angiotensin ii-induced cardiac inflammation and fibrosis by blocking Nlrp3 inflammasome activation, Biochim. Biophys. Acta 1864 (2018) 1–10.
[27] B. Vandanmagsar, Y.H. Youm, A. Ravussin, J.E. Galgani, K. Stadler, R.L. Mynatt, E. Ravussin, J.M. Stephens, V.D. Dixit, The Nlrp3 inflammasome instigates obesity-induced inflammation and insulin resistance, Nat. Med. 17 (2011) 179–188.
[28] T. Jourdan, G. Godlewski, R. Cinar, A. Bertola, G. Szanda, J. Liu, J. Tam, T. Han, B. Mukhopadhyay, M.C. Skarulis, C. Ju, M. Aouadi, M.P. Czech, G. Kunos, Activation of the Nlrp3 inflammasome in infiltrating macrophages by endocannabinoids mediates beta cell loss in type 2 diabetes, Nat. Med. 19 (2013) 1132–1140.
[29] B.D. Paul, S.H. Snyder, H2s: a novel gasotransmitter that signals by sulfhydration, Trends Biochem. Sci. 40 (2015) 687–700.
[30] D.J. Polhemus, D.J. Lefer, Emergence of hydrogen sulfide as an endogenous gaseous signaling molecule in cardiovascular disease, Circ. Res. 114 (2014) 730–737.
[31] C.W. Huang, P.K. Moore, H2s synthesizing enzymes: biochemistry and molecular aspects, Handb. Exp. Pharmacol. 230 (2015) 3–25.
[32] N. Tyagi, K.S. Moshal, U. Sen, T.P. Vacek, M. Kumar, W.M. Hughes Jr., S. Kundu, S.C. Tyagi, H2s protects against methionine-induced oxidative stress in brain endothelial cells, Antioxid. Redox Signal. 11 (2009) 25–33.
[33] D. Wu, Q. Hu, X. Liu, L. Pan, Q. Xiong, Y.Z. Zhu, Hydrogen sulfide protects against apoptosis under oxidative stress through Sirt1 pathway in H9c2 cardiomyocytes, Nitric Oxide 46 (2015) 204–212.
[34] M. Hu, W. Zou, C.Y. Wang, X. Chen, H.Y. Tan, H.Y. Zeng, P. Zhang, H.F. Gu, X.Q. Tang, Hydrogen sulfide protects against chronic unpredictable mild stress-induced oxidative stress in hippocampus by upregulation of Bdnf-Trkb pathway, Oxidative Med. Cell. Longev. 2016 (2016) 2153745.
[35] A.K. Mustafa, M.M. Gadalla, N. Sen, S. Kim, W. Mu, S.K. Gazi, R.K. Barrow, G. Yang, R. Wang, S.H. Snyder, H2s signals through protein S-sulfhydration, Sci. Signal. 2 (2009) ra72.
[36] G. Meng, J. Zhu, Y. Xiao, Z. Huang, Y. Zhang, X. Tang, L. Xie, Y. Chen, Y. Shao, A. Ferro, R. Wang, P.K. Moore, Y. Ji, Hydrogen sulfide donor Gyy4137 protects against myocardial fibrosis, Oxidative Med. Cell. Longev. 2015 (2015) 691070.
[37] L. Xie, H. Feng, S. Li, G. Meng, S. Liu, X. Tang, Y. Ma, Y. Han, Y. Xiao, Y. Gu, Y. Shao, C.M. Park, M. Xian, Y. Huang, A. Ferro, R. Wang, P.K. Moore, H. Wang, Y. Ji, Sirt3 mediates the antioxidant effect of hydrogen sulfide in endothelial cells, Antioxid. Redox Signal. 24 (2016) 329–343.
[38] L. Xie, Y. Gu, M. Wen, S. Zhao, W. Wang, Y. Ma, G. Meng, Y. Han, Y. Wang, G. Liu, P.K. Moore, X. Wang, H. Wang, Z. Zhang, Y. Yu, A. Ferro, Z. Huang, Y. Ji, Hydrogen sulfide induces Keap1 S-sulfhydration and suppresses diabetes-accelerated atherosclerosis via Nrf2 activation, Diabetes 65 (2016) 3171–3184.
[39] G. Meng, Y. Xiao, Y. Ma, X. Tang, L. Xie, J. Liu, Y. Gu, Y. Yu, C.M. Park, M. Xian, X. Wang, A. Ferro, R. Wang, P.K. Moore, Z. Zhang, H. Wang, Y. Han, Y. Ji, Hydrogen sulfide regulates Kruppel-like factor 5 transcription activity via specificity protein 1 S-sulfhydration at Cys664 to prevent myocardial hypertrophy, J. Am. Heart Assoc. 5 (2016).
[40] J. Wang, W. Wang, S. Li, Y. Han, P. Zhang, G. Meng, Y. Xiao, L. Xie, X. Wang, J. Sha, Q. Chen, P.K. Moore, R. Wang, W. Xiang, Y. Ji, Hydrogen sulfide as a potential target in preventing spermatogenic failure and testicular dysfunction, Antioxid. Redox Signal. 28 (2018) 1447–1462.
[41] V. Tarallo, Y. Hirano, B.D. Gelfand, S. Dridi, N. Kerur, Y. Kim, W.G. Cho, H. Kaneko, B.J. Fowler, S. Bogdanovich, R.J. Albuquerque, W.W. Hauswirth, V.A. Chiodo, J.F. Kugel, J.A. Goodrich, S.L. Ponicsan, G. Chaudhuri, M.P. Murphy, J.L. Dunaief, B.K. Ambati, Y. Ogura, J.W. Yoo, D.K. Lee, P. Provost, D.R. Hinton, G. Nunez,

J.Z. Baffi, M.E. Kleinman, J. Ambati, Dicer1 loss and Alu Rna induce age-related macular degeneration via the Nlrp3 inflammasome and Myd88, Cell 149 (2012) 847–859.
[42] Y. Ju, A. Untereiner, L. Wu, G. Yang, H2s-induced S-sulfhydration of pyruvate carboxylase contributes to gluconeogenesis in liver cells, Biochim. Biophys. Acta 1850 (2015) 2293–2303.
[43] J. Weischenfeldt, B. Porse, Bone Marrow-Derived Macrophages (Bmm): Isolation and Applications, 2008 CSH Protoc, 2008 (pdb prot5080).
[44] J.J. Kotzin, S.P. Spencer, S.J. Mccright, D.B.U. Kumar, M.A. Collet, W.K. Mowel, E.N. Elliott, A. Uyar, M.A. Makiya, M.C. Dunagin, C.C.D. Harman, A.T. Virtue, S. Zhu, W. Bailis, J. Stein, C. Hughes, A. Raj, E.J. Wherry, L.A. Goff, A.D. Klion, J.L. Rinn, A. Williams, R.A. Flavell, J. Henao-Mejia, The long non-coding Rna Morrbid regulates Bim and short-lived myeloid cell lifespan, Nature 537 (2016) 239–243.
[45] Z. Liu, Y. Han, L. Li, H. Lu, G. Meng, X. Li, M. Shirhan, M.T. Peh, L. Xie, S. Zhou, X. Wang, Q. Chen, W. Dai, C.H. Tan, S. Pan, P.K. Moore, Y. Ji, The hydrogen sulfide donor, Gyy4137, exhibits anti-atherosclerotic activity in high fat fed apolipoprotein E(−/−) mice, Br. J. Pharmacol. 169 (2013) 1795–1809.
[46] E. Pomari, B. Stefanon, M. Colitti, Effect of plant extracts on H2o2-induced inflammatory gene expression in macrophages, J. Inflamm. Res. 7 (2014) 103–112.
[47] J. Dan Dunn, L.A. Alvarez, X. Zhang, T. Soldati, Reactive oxygen species and mitochondria: a nexus of cellular homeostasis, Redox Biol. 6 (2015) 472–485.
[48] H. Li, S. Horke, U. Forstermann, Vascular oxidative stress, nitric oxide and atherosclerosis, Atherosclerosis 237 (2014) 208–219.
[49] Y. Jiang, M. Wang, K. Huang, Z. Zhang, N. Shao, Y. Zhang, W. Wang, S. Wang, Oxidized low-density lipoprotein induces secretion of interleukin-1beta by macrophages via reactive oxygen species-dependent Nlrp3 inflammasome activation, Biochem. Biophys. Res. Commun. 425 (2012) 121–126.
[50] C.F. Lee, M. Qiao, K. Schroder, Q. Zhao, R. Asmis, Nox4 is a novel inducible source of reactive oxygen species in monocytes and macrophages and mediates oxidized low density lipoprotein-induced macrophage death, Circ. Res. 106 (2010) 1489–1497.
[51] A.J. Freemerman, A.R. Johnson, G.N. Sacks, J.J. Milner, E.L. Kirk, M.A. Troester, A.N. Macintyre, P. Goraksha-Hicks, J.C. Rathmell, L. Makowski, Metabolic reprogramming of macrophages: glucose transporter 1 (Glut1)-mediated glucose metabolism drives a proinflammatory phenotype, J. Biol. Chem. 289 (2014) 7884–7896.
[52] Z.J. Wang, J.H. Xie, L.J. Kan, J.Q. Wang, M.Y. Shen, W.J. Li, S.P. Nie, M.Y. Xie, Sulfated polysaccharides from cyclocarya paliurus reduce H2o2-induced oxidative stress in Raw264.7 cells, Int. J. Biol. Macromol. 80 (2015) 410–417.
[53] F.J. Roca, L. Ramakrishnan, Tnf dually mediates resistance and susceptibility to mycobacteria via mitochondrial reactive oxygen species, Cell 153 (2013) 521–534.
[54] E. Vergadi, M.S. Chang, C. Lee, O.D. Liang, X. Liu, A. Fernandez-Gonzalez, S.A. Mitsialis, S. Kourembanas, Early macrophage recruitment and alternative activation are critical for the later development of hypoxia-induced pulmonary hypertension, Circulation 123 (2011) 1986–1995.
[55] M. Giorgio, M. Trinei, E. Migliaccio, P.G. Pelicci, Hydrogen peroxide: a metabolic by-product or a common mediator of ageing signals? Nat. Rev. Mol. Cell Biol. 8 (2007) 722–728.
[56] W.W. Chao, Y.C. Chung, I.P. Shih, H.Y. Wang, S.T. Chou, C.K. Hsu, Red bean extract inhibits lipopolysaccharide-induced inflammation and H(2)O(2)-induced oxidative stress in raw 264.7 macrophages, J. Med. Food 18 (2015) 724–730.
[57] S. Shimizu, R. Yonezawa, T. Hagiwara, T. Yoshida, N. Takahashi, S. Hamano, T. Negoro, T. Toda, M. Wakamori, Y. Mori, M. Ishii, Inhibitory effects of Ag490 on H2o2-induced Trpm2-mediated Ca(2+) entry, Eur. J. Pharmacol. 742 (2014) 22–30.
[58] H. Zhao, P. Pan, Y. Yang, H. Ge, W. Chen, J. Qu, J. Shi, G. Cui, X. Liu, H. Feng, Y. Chen, Endogenous hydrogen sulphide attenuates Nlrp3 inflammasome-mediated neuroinflammation by suppressing the P2x7 receptor after intracerebral haemorrhage in rats, J. Neuroinflammation 14 (2017) 163.
[59] Z.L. Luo, J.D. Ren, Z. Huang, T. Wang, K. Xiang, L. Cheng, L.J. Tang, The role of exogenous hydrogen sulfide in free fatty acids induced inflammation in macrophages, Cell. Physiol. Biochem. 42 (2017) 1635–1644.
[60] M. Castelblanco, J. Lugrin, D. Ehirchiou, S. Nasi, I. Ishii, A. So, F. Martinon, N. Busso, Hydrogen sulfide inhibits Nlrp3 inflammasome activation and reduces cytokine production both in vitro and in a mouse model of inflammation, J. Biol. Chem. 293 (2018) 2546–2557.
[61] J.M. Abais, M. Xia, Y. Zhang, K.M. Boini, P.L. Li, Redox regulation of Nlrp3 inflammasomes: Ros as trigger or effector? Antioxid. Redox Signal. 22 (2015) 1111–1129.
[62] M.E. Heid, P.A. Keyel, C. Kamga, S. Shiva, S.C. Watkins, R.D. Salter, Mitochondrial reactive oxygen species induces Nlrp3-dependent lysosomal damage and inflammasome activation, J. Immunol. 191 (2013) 5230–5238.
[63] Y. Wang, G.Z. Wang, P.S. Rabinovitch, I. Tabas, Macrophage mitochondrial oxidative stress promotes atherosclerosis and nuclear factor-kappab-mediated inflammation in macrophages, Circ. Res. 114 (2014) 421–433.
[64] F. Usui, K. Shirasuna, H. Kimura, K. Tatsumi, A. Kawashima, T. Karasawa, K. Yoshimura, H. Aoki, H. Tsutsui, T. Noda, J. Sagara, S. Taniguchi, M. Takahashi, Inflammasome activation by mitochondrial oxidative stress in macrophages leads to the development of angiotensin ii-induced aortic aneurysm, Arterioscler. Thromb. Vasc. Biol. 35 (2015) 127–136.
[65] M.R. Filipovic, Persulfidation (S-sulfhydration) and H2s, Handb. Exp. Pharmacol. 230 (2015) 29–59.
[66] S. Mir, T. Sen, N. Sen, Cytokine-induced Gapdh sulfhydration affects Psd95 degradation and memory, Mol. Cell 56 (2014) 786–795.
[67] N. Sen, B.D. Paul, M.M. Gadalla, A.K. Mustafa, T. Sen, R. Xu, S. Kim, S.H. Snyder, Hydrogen sulfide-linked sulfhydration of Nf-kappab mediates its antiapoptotic actions, Mol. Cell 45 (2012) 13–24.
[68] M. Iciek, D. Kowalczyk-Pachel, A. Bilska-Wilkosz, I. Kwiecien, M. Gorny, L. Wlodek, S-Sulfhydration as a cellular redox regulation, Biosci. Rep. 36 (2015).
[69] N. Krishnan, C. Fu, D.J. Pappin, N.K. Tonks, H2s-induced sulfhydration of the phosphatase Ptp1b and its role in the endoplasmic reticulum stress response, Sci. Signal. 4 (2011) ra86.
[70] N.R. Sundaresan, M. Gupta, G. Kim, S.B. Rajamohan, A. Isbatan, M.P. Gupta, Sirt3 blocks the cardiac hypertrophic response by augmenting Foxo3a-dependent antioxidant defense mechanisms in mice, J. Clin. Invest. 119 (2009) 2758–2771.
[71] J. Traba, M. Kwarteng-Siaw, T.C. Okoli, J. Li, R.D. Huffstutler, A. Bray, M.A. Waclawiw, K. Han, M. Pelletier, A.A. Sauve, R.M. Siegel, M.N. Sack, Fasting and refeeding differentially regulate Nlrp3 inflammasome activation in human subjects, J. Clin. Invest. 125 (2015) 4592–4600.
[72] J. Traba, S.S. Geiger, M. Kwarteng-Siaw, K. Han, O.H. Ra, R.M. Siegel, D. Gius, M.N. Sack, Prolonged fasting suppresses mitochondrial Nlrp3 inflammasome assembly and activation via Sirt3-mediated activation of superoxide dismutase 2, J. Biol. Chem. 292 (2017) 12153–12164.
[73] D. Bellizzi, G. Covello, F. Di Cianni, Q. Tong, G. De Benedictis, Identification of Gata2 and Ap-1 activator elements within the enhancer Vntr occurring in intron 5 of the human Sirt3 gene, Mol. Cell 28 (2009) 87–92.
[74] Y. Zhou, A.C.K. Chung, R. Fan, H.M. Lee, G. Xu, B. Tomlinson, J.C.N. Chan, A.P.S. Kong, Sirt3 deficiency increased the vulnerability of pancreatic beta cells to oxidative stress-induced dysfunction, Antioxid. Redox Signal. 27 (2017) 962–976.
[75] M. Komatsu, S. Kageyama, Y. Ichimura, P62/Sqstm1/A170: physiology and pathology, Pharmacol. Res. 66 (2012) 457–462.
[76] Z. Zhong, A. Umemura, E. Sanchez-Lopez, S. Liang, S. Shalapour, J. Wong, F. He, D. Boassa, G. Perkins, S.R. Ali, M.D. Mcgeough, M.H. Ellisman, E. Seki, A.B. Gustafsson, H.M. Hoffman, M.T. Diaz-Meco, J. Moscat, M. Karin, Nf-Kappab restricts inflammasome activation via elimination of damaged mitochondria, Cell 164 (2016) 896–910.
[77] T. Ishii, E. Warabi, R.C. Siow, G.E. Mann, Sequestosome1/P62: a regulator of redox-sensitive voltage-activated potassium channels, arterial remodeling, inflammation, and neurite outgrowth, Free Radic. Biol. Med. 65 (2013) 102–116.
[78] A. Jain, T. Lamark, E. Sjottem, K.B. Larsen, J.A. Awuh, A. Overvatn, M. Mcmahon, J.D. Hayes, T. Johansen, P62/Sqstm1 is a target gene for transcription factor Nrf2 and creates a positive feedback loop by inducing antioxidant response element-driven gene transcription, J. Biol. Chem. 285 (2010) 22576–22591.
[79] N. Rubio, J. Verrax, M. Dewaele, T. Verfaillie, T. Johansen, J. Piette, P. Agostinis, P38(Mapk)-regulated induction of P62 and Nbr1 after photodynamic therapy promotes autophagic clearance of ubiquitin aggregates and reduces reactive oxygen species levels by supporting Nrf2-antioxidant signaling, Free Radic. Biol. Med. 67 (2014) 292–303.
[80] J.A. Pan, Y. Sun, Y.P. Jiang, A.J. Bott, N. Jaber, Z. Dou, B. Yang, J.S. Chen, J.M. Catanzaro, C. Du, W.X. Ding, M.T. Diaz-Meco, J. Moscat, K. Ozato, R.Z. Lin, W.X. Zong, Trim21 ubiquitylates Sqstm1/P62 and suppresses protein sequestration to regulate redox homeostasis, Mol. Cell 61 (2016) 720–733.
[81] A. Puissant, G. Robert, N. Fenouille, F. Luciano, J.P. Cassuto, S. Raynaud, P. Auberger, Resveratrol promotes autophagic cell death in chronic myelogenous leukemia cells via Jnk-mediated P62/Sqstm1 expression and Ampk activation, Cancer Res. 70 (2010) 1042–1052.
[82] Y.T. Tung, B.J. Wang, W.M. Hsu, M.K. Hu, G.M. Her, W.P. Huang, Y.F. Liao, Presenilin-1 regulates the expression of P62 to govern P62-dependent Tau degradation, Mol. Neurobiol. 49 (2014) 10–27.
[83] J. Ling, Y. Kang, R. Zhao, Q. Xia, D.F. Lee, Z. Chang, J. Li, B. Peng, J.B. Fleming, H. Wang, J. Liu, I.R. Lemischka, M.C. Hung, P.J. Chiao, Krasg12d-induced Ikk2/Beta/Nf-kappab activation by Il-1alpha and P62 feedforward loops is required for development of pancreatic ductal adenocarcinoma, Cancer Cell 21 (2012) 105–120.
[84] M.R. Hellmich, C. Szabo, Hydrogen sulfide and cancer, Handb. Exp. Pharmacol. 230 (2015) 233–241.
[85] J. Beltowski, Hydrogen sulfide in pharmacology and medicine—an update, Pharmacol. Rep. 67 (2015) 647–658.